Research Article | Vol. 14, No. 8 / 1 Aug 2024 / Optical Materials Express 1933

Optical Materials EXPRESS

On the thermal stability of multilayer optics for use with high X-ray intensities

MARGARITA ZAKHAROVA,[1] ZLATKO REK,[2] BOŽIDAR ŠARLER,[2,3] AND SAŠA BAJT[1,4,*]

[1] Center for Free-Electron Laser Science CFEL, Deutsches Elektronen-Synchrotron DESY, Notkestr. 85, 22607 Hamburg, Germany

[2] Laboratory for Fluid Dynamics and Thermodynamics, Faculty of Mechanical Engineering, University of Ljubljana, Aškerčeva 6, 1000 Ljubljana, Slovenia

[3] Laboratory for Simulation of Materials and Processes, Institute of Metals and Technology, Lepi pot 11, 1000 Ljubljana, Slovenia

[4] The Hamburg Centre for Ultrafast Imaging, Universität Hamburg, Luruper Chaussee 149, 227619 Hamburg, Germany

[*] sasa.bajt@desy.de

Abstract: High-intensity X-ray free electron laser (XFEL) beams require optics made of materials with minimal radiation absorption, high diffraction efficiency, and high radiation hardness. Multilayer Laue lenses (MLLs) are diffraction-based X-ray optics that can focus XFEL beams, as already demonstrated with tungsten carbide/silicon carbide (WC/SiC)-based MLLs. However, high atomic number materials such as tungsten strongly absorb X-rays, resulting in high heat loads. Numerical simulations predict much lower heat loads in MLLs consisting of low atomic number Z materials, although such MLLs have narrower rocking curve widths. In this paper, we first screen various multilayer candidates and then focus on Mo_2C/SiC multilayer due to its high diffraction efficiency. According to numerical simulations, the maximum temperature in this multilayer should remain below 300°C if the MLL made out of this multilayer is exposed to an XFEL beam of 17.5 keV photon energy, 1 mJ energy per pulse and 10 kHz pulse repetition rate. To understand the thermal stability of the Mo_2C/SiC multilayer, we performed a study on the multilayers of three different periods (1.5, 5, and 12 nm) and different Mo_2C to SiC ratios. We monitored their periods, crystallinity, and stress as a function of annealing temperature for two different heating rates. The results presented in this paper indicate that Mo_2C/SiC-based MLLs are viable for focusing XFEL beams without being damaged under these conditions.

Published by Optica Publishing Group under the terms of the Creative Commons Attribution 4.0 License. Further distribution of this work must maintain attribution to the author(s) and the published article's title, journal citation, and DOI.

1. Introduction

X-ray free electron lasers (XFELs) generate intense, pulsed, and coherent X-ray beams that have revolutionized numerous applications and opened up new scientific fields. For example, they enabled the measurement of atomically-resolved structural dynamics in macromolecules and compounds, a better understanding of high-energy-density physics and non-linear X-ray optics [1–3]. However, the manipulation of XFEL beams is very challenging and puts stringent requirements on X-ray optics. Optical components can be easily damaged or even destroyed when exposed to their full intensity. High repetition rates of XFELs also significantly increase the thermal load for X-ray optics and can impair their functionality [4]. Focusing of XFEL beams is usually done with beryllium compound refractive lenses [5] and grazing incidence reflective mirrors [6]. However, aforementioned challenges sparked interest in developing and testing other types of optics, including diamond-based Fresnel zone plates [7], multilayer-coated Kirkpatrick-Baez mirrors [8] and multilayer Laue lenses (MLLs) [9].

#527226
Journal © 2024

https://doi.org/10.1364/OME.527226
Received 10 Apr 2024; accepted 21 Jun 2024; published 2 Jul 2024

The MLLs are a relatively new type of X-ray diffractive optics that are based on multilayers [10]. Similarly to the Fresnel zone plate, the diffraction angle in an MLL is determined by the thickness of the layers at a certain position in the lens and the wavelength of the incident radiation. The layer thickness varies according to the zone plate law and gets smaller with increasing distance from the optical axis such that all the diffracted rays end up in a common focus. To make an efficient lens, the layers in each position along the lens have to be correctly tilted or curved to simultaneously obey Bragg's law, $\theta_n = \lambda/(2d_n)$ [11]. One way to achieve such curved layers is by placing a straight mask above the substrate during the deposition [12,13]. These lenses can consist of tens of thousands of alternating layers, which are usually deposited using magnetron sputtering, and depositions can take a week or longer. During this process, errors in the layer placement accumulate over time and lead to aberrations, which need to be minimized. The overall multilayer height is limited by the number of layers one can deposit without any interruption, the ultimate reason being the consumption of the sputtering targets. Other factors, such as stress and roughness, have to be considered as well. Nevertheless, MLLs taller than 100 microns have been demonstrated [9,14]. MLLs are prepared by slicing the prepared multilayer perpendicular to the layer growth direction. In a subsequent step, they are thinned to the optimal optical depth (thickness in the beam propagation direction). This optical depth depends on the energy at which the lens is to be used and on the multilayer materials. Slicing and thinning are done with a focused ion beam since mechanical processing is known to produce external stresses and leads to film fracture due to the interface delamination or cracking [15].

The MLLs, which were previously used to focus an XFEL beam [9], were based on tungsten carbide/silicon carbide (WC/SiC) multilayers. These multilayers could withstand an incident fluence of approximately 0.13 J/cm^2 per pulse for up to 30 pulses per train with 23.5% transmission. However, when exposed to even higher pulse-per-train frequencies, the lenses detached from the substrate. Numerical simulations confirmed that using lower atomic number (Z) material pairs such as B_4C/SiC, TiC/SiC, or Be/SiC could significantly lower the heat load for a given incident pulse energy and pulse repetition rate [16]. This is primarily due to lower absorption, which also necessitates lenses with larger optical depth to achieve optimum diffraction efficiency. Thus, the lens has a larger volume in which the heat is distributed. The same approach can be extended to various types of optics utilized at XFEL facilities. For instance, increasing the crystal volume of Bragg reflectors has been proposed as a means to alleviate strain caused by thermoelastic effects [4,17]. The detachment of the MLLs from their mounts in the aforementioned experiment was likely caused by significant stress changes due to extreme temperature gradients [16], a result of substantial absorption in tungsten carbide.

To find suitable materials that could be used to prepare MLLs in the future, we explored different multilayer candidates consisting of materials of low atomic number Z. In addition to their high thermal and radiation stability, we have to consider that these materials should form high-quality multilayer structures for a broad range of layer thicknesses needed in MLLs. We first calculated diffraction efficiencies and relative bandwidths of several material pairs (Al/SiC, B_4C/SiC, Cr/SiC, Mo_2C/SiC) and compared them with multilayers that are frequently used to prepare MLLs (WSi_2/Al, WSi_2/Si, and WC/SiC). The most promising candidate, Mo_2C/SiC multilayer, was then studied in more detail. First, we performed numerical simulations of the heat load (maximum and average temperatures) in Mo_2C/SiC and also in WC/SiC assuming XFEL photon energy of 17.5 keV and 1 mJ energy per pulse for two different XFEL pulse repetition rates. We then prepared Mo_2C/SiC multilayers of three different periods (1.5, 5, and 12 nm) and three Γ values, where Γ is defined as a ratio of the thickness of the material with high atomic number Z (e.g. Mo_2C) to the multilayer period thickness. The three Γ values considered here were 0.3, 0.5 and 0.7. We studied Mo_2C/SiC multilayers and measured their period, microstructure and stress as a function of annealing temperature.

Optical Materials EXPRESS

2. Screening multilayer material pairs

The diffraction efficiency of a multilayer in the symmetric Laue geometry is described by dynamical diffraction [18,19]. Within the multilayer structure the beam is split into two components—one that is undeflected and one that is reflected by $2\theta_n$. It is this reflected beam that forms the focus. The energy partitioned into the focused beam increases as the optical depth of the MLL is increased from zero, with a corresponding decrease in the undeflected intensity. In the absence of absorption, the focusing efficiency reaches a maximum at half of the so-called pendellösung period given by

$$\tau_{\mathrm{opt}} = \frac{\pi\lambda\cos\theta_n}{4\,\Delta n\,\sin\pi\Gamma} \tag{1}$$

for a wavelength λ and a difference Δn of refractive indices of the layer materials [20]. Most MLL systems developed so far have used material pairs with a large refractive difference, consisting of a dense material (the "absorber" layer) and a light material (the "spacer" layer). While this ensures small optical depths, it does not necessarily minimize absorption in the structure. The approach of a thick, light, low-contrast MLL does come at the cost of a reduced rocking curve width, which is given by [18]

$$\Delta\theta \approx \frac{|\Delta n|\sin\pi\Gamma}{\pi\,\theta_n} \tag{2}$$

and a corresponding bandwidth

$$\frac{\Delta\lambda}{\lambda} \approx \frac{|\Delta n|\sin\pi\Gamma}{\pi\,\theta_n^2}. \tag{3}$$

We calculated the optimal optical depths and corresponding theoretically achievable diffraction efficiencies and bandwidths for MLLs made of different material pairs. Diffraction efficiencies [18] are shown in Fig. 1(a) and their relative bandwidths are presented in Fig. 1(b). The calculations were done for periodic multilayers (10 nm) at 17.5 keV photon energy using refractive indices of relevant materials retrieved from xraylib library [21]. As can be seen, multilayers with materials of low atomic number Z outperform multilayers that contain tungsten and are commonly used in MLLs [10,14,18] in terms of efficiency. Among them, B_4C/SiC has the highest theoretical diffraction efficiency, followed by Mo_2C/SiC. Even though the bandwidths of these lower contrast material pairs are narrower than the bandwidths of commonly used materials for MLLs, they are still larger than the SASE XFEL beam relative bandwidth of 10^{-3} [2].

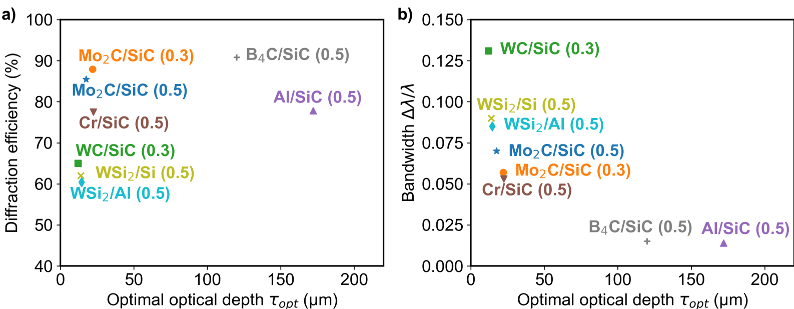

Fig. 1. Calculated theoretical diffraction efficiencies (a) and bandwidths (b) of different multilayers assuming a period thickness of 10 nm and Γ values indicated in the brackets. All the calculations were done for the photon energy of 17.5 keV using dynamic diffraction theory.

However, high diffraction efficiency is just one of the properties to consider. The other requirements include interface sharpness and smoothness, intrinsic stress, and thermal stability

of the multilayer. The stress is inevitably introduced during the multilayer deposition and can be quite high, especially for thicker coatings. The overall shear force imposed on the substrate grows proportionally with the coating thickness and its stress. The multilayer's intrinsic stress and adhesion strength set the limit of the achievable multilayer thickness without cracking or delamination from the substrate [22]. The stress can be modified by changing the ratio between the two materials or by varying the deposition parameters (e.g., gas type and pressure) [23,24]. This approach is usually exploited when growing tall multilayer stacks. However, some material pairs exhibit high intrinsic stress, which cannot be substantially mitigated with varying deposition parameters.

The considerations mentioned above entail that multilayer material pairs have low intrinsic stress. Based on this requirement, B_4C/SiC multilayers were not considered further in this study, despite their high diffraction efficiency and low absorption. High stress in B_4C/SiC leads to delamination or cracking of the multilayer and also makes any post-deposition processing (e.g., cutting) extremely challenging.

In Cr/SiC multilayers, strong intermixing between Cr and SiC was observed already in an as-deposited state, and this intermixing increased with annealing temperature. Annealing to 300°C led to substantial changes in the multilayer period (>1%), rendering Cr/SiC multilayers unsuitable for further study.

In the case of Al/SiC multilayers, high interface roughness led to their dismissal from further study. While the crystallinity of Al layers can be suppressed by using nitrogen as a sputtering gas [25], this approach tested by us proved ineffective for larger periods. Additionally, Al/SiC is thermally unstable. For example, we observed that annealing at 300°C for 1 hour caused unacceptable period (Λ) contractions of 1% for a multilayer with a period of $\Lambda \approx 17$ nm and $\Gamma = 0.5$ and 3% for $\Lambda \approx 15$ nm and $\Gamma = 0.3$. Such changes in period contraction would misplace the layers in the MLL structure, resulting in wavefront aberrations. Numerical simulations predict that changes in the layer thickness (both stochastic and systematic) deteriorate the focusing performance of the MLL by decreasing the intensity of the focused beam and lead to the appearance of satellite peaks [26,27].

WC/SiC with $\Gamma = 0.5$ exhibited high heat load in previous XFEL experiments [9]. However, since WC/SiC has otherwise exceptionally good multilayer properties [11,28–30], we nevertheless included calculations of WC/SiC with $\Gamma = 0.3$ in our study.

Following our initial screening, Mo_2C/SiC multilayer emerged as the most promising candidate. This outcome might not appear surprising given the widespread use of Mo/Si-based multilayers for high-quality EUV optics and the known enhancement of reflectivity [31,32] and thermal stability [33] with the addition of thin carbon layers on the interfaces. An amorphous-to-crystalline transition, which typically occurs in pure Mo just above 2 nm layer thickness [34], is expected to be suppressed and shifted towards thicker layers. Previous studies on Mo_2C-containing multilayers [35] also suggest smooth and sharp interfaces and high thermal stability.

2.1. Numerical simulations of the heat load

Previously reported dynamic thermoelastic simulations indicated that the finite heat transfer between the optics and the holder notably increases the optics temperature, and is important to consider when simulating the heat load induced by XFELs with MHz repetition rates [17]. *Rek et al.* [16] performed numerical simulations of the heat load in multilayers of various material pairs and geometrical designs considered for MLLs. These simulations also showed that the mounting geometry of the MLL lenses has an impact on thermal load. Large surface contact between the MLL and highly conductive and thermally stable material, like diamond, is advantageous to accelerate heat dissipation. Sturdy mounting also makes the overall structure more robust. However, to lower the heat loads in MLLs the choice of multilayer materials is even more critical than the mounting geometry.

Optical Materials EXPRESS

The study [16] also revealed that materials of low atomic number Z such as Be/SiC or B_4C/SiC should be able to accept a full beam of about 10 J/cm^2 fluence even for MHz repetition rate. To minimize the heat load and thus reduce the absorbed dose, it is advantageous to maximize the MLL volume. For the same MLL design and X-ray energy, the optimal optical depth for materials of low atomic number Z is larger, and the heat load can spread over a larger volume. With a lower absorbed dose, the temperature increase is smaller, easing the demands on thermal stability. However, due to Be toxicity and high stress in B_4C/SiC these were not considered here.

Here, we calculated heat loads on Mo_2C/SiC multilayers with Γ of 0.5 and 0.3, and WC/SiC multilayer with Γ = 0.3 assuming 17.5 keV photon energy, 1 mJ energy per pulse, for two different times between successive pulses, $\Delta t = 3.6\ \mu$s and $\Delta t = 100\ \mu$s. Calculated average and maximum temperatures shown in Table 1 and Fig. 2 for two Δt demonstrate strong dependence on the pulse repetition rate.

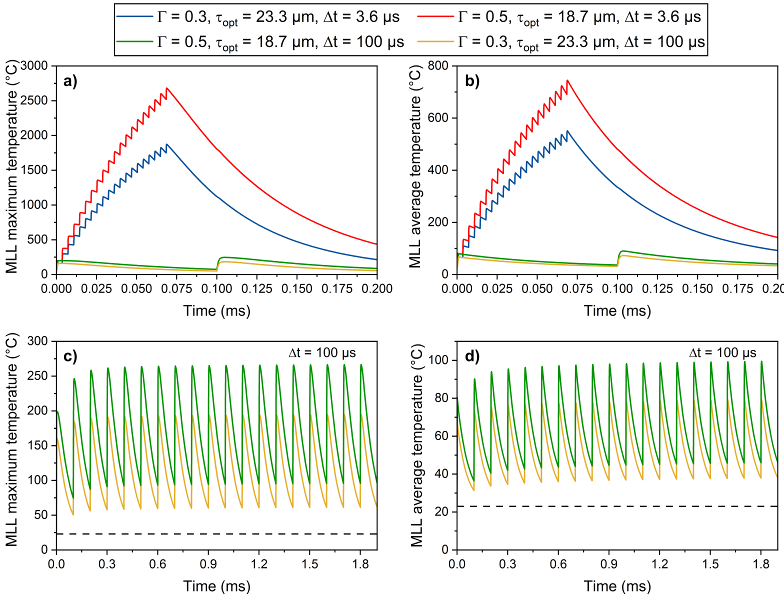

Fig. 2. Maximum (a, c) and average (b, d) temperature results obtained with numerical simulations for Mo_2C/SiC with Γ = 0.3 and 0.5 considering $\Delta t = 3.6\ \mu$s and $\Delta t = 100\ \mu$s between successive pulses. The photon energy of 17.5 keV was assumed. The gray dashed line indicates the room temperature (23 °C).

Table 1. The average T_{avg} and maximum T_{max} temperatures (in °C) for Mo_2C/SiC MLLs (Γ = 0.3 and Γ = 0.5) and WC/SiC (Γ = 0.3) exposed to X-rays with photon energy of 17.5 keV, 1 mJ energy per pulse and for $\Delta t = 100\ \mu$s and $\Delta t = 3.6\ \mu$s time intervals between two successive pulses

	$\Delta t = 100\ \mu$s		$\Delta t = 3.6\ \mu$s	
Multilayer	T_{max}	T_{avg}	T_{max}	T_{avg}
Mo_2C/SiC, Γ = 0.3	195	79	1874	551
Mo_2C/SiC, Γ = 0.5	267	100	2682	745
WC/SiC, Γ = 0.3	564	195	8090	2123

Figure 2 illustrates the time evolution of the simulated maximum (a, c) and average (b, d) temperature for Mo_2C/SiC-based MLL after 20 X-ray pulses. The green and yellow curves represent the case when the pulses are separated by 100 μs for two different optical depths,

Optical Materials EXPRESS

corresponding to Γ = 0.3 (yellow) and Γ = 0.5 (green). In Fig. 2(a-b), the case for 20 X-ray pulses separated by 3.6 μs is shown for these two MLL designs with Γ = 0.3 (blue) and Γ = 0.5 (red). In the case of a faster pulse repetition rate (Δt = 3.6 μs or 0.27 MHz) the maximum temperature in the multilayer with Γ = 0.5 reaches 2682°C. The maximum temperature in the multilayer with Γ = 0.3 is lower (1874°C) but still too high for any practical application. Table 1 shows also maximum and average temperatures in WC/SiC multilayers with Γ = 0.3. Under the same conditions, this multilayer would be immediately destroyed (maximum temperature is 8090°C). However, for a lower repetition rate (10 kHz), there is enough time for the multilayer to cool down in between pulses, so the temperatures are much lower. For example, in Mo_2C/SiC the maximum temperatures are 267°C for Γ = 0.5 and 195°C for Γ = 0.3. The maximum temperature in WC/SiC multilayer with Γ = 0.3 is predicted to reach 564°C.

The numerical simulations were conducted in a similar manner to those reported previously by *Rek et al.* [16], where the multilayer structure with nanometer layers was simulated as a slab made of two materials in the proportion indicated by Γ. For example, in a Mo_2C/SiC multilayer with Γ = 0.3, the slab would contain 30% Mo_2C and 70% SiC. This way, we approximate the thermal properties of the multilayer structure as the average of the individual components. We use them to predict the temperature rise in the MLLs under specific XFEL beam conditions.

3. Thermal stability of the molybdenum carbide/silicon carbide multilayer

3.1. Sample preparation and characterization

All coatings were deposited in our laboratory at DESY using magnetron sputtering [11] technique. The depositions were done in a vacuum system with four magnetrons placed 90 degrees apart using Krypton (1.5 mTorr) as a sputtering gas. The depositions were done using constant power. The power on Mo_2C was kept at 100 W and on SiC at 220 W. We prepared three sets of Mo_2C/SiC samples. The first set, which consisted of Mo_2C/SiC multilayers with a period of 5 nm and Γ = 0.3 and 0.5 was annealed to 300°C and 700°C with a slow heating rate. The second set consisted of Mo_2C/SiC multilayers with periods of 1.5, 5, and 12 nm and Γ = 0.3, 0.5, 0.7 and was used to study stress changes for temperatures from 70°C up to 300°C. The third set, which also consisted of Mo_2C/SiC multilayers with periods of 1.5, 5, and 12 nm and Γ = 0.3, 0.5, 0.7 was used for cycled annealing to 250°C with a fast heating rate. Individual monolayers of Mo_2C (86.3 ± 1 nm) and SiC (99 ± 1 nm) were prepared as well.

Multilayers and monolayers were deposited on Si (100) substrates with a surface roughness of 0.15 nm. The substrates were placed on a substrate holder, which spun during the deposition. The thickness of the layers was controlled with the platter velocity (sputtering time). The range of period thicknesses (1.5 to 12 nm) studied here corresponds to a typical range of periods in a high-resolution MLL.

After the deposition, the samples were measured using small-angle X-ray diffraction (SAXRD) to determine their periods, while the microstructure was determined using high-angle X-ray diffraction (HAXRD). These measurements were carried out with X'Pert Pro MRD (Panalytical, The Netherlands) using Cu K-α radiation (0.15418 nm). The SAXRD measurements were fitted with IMD software [36]. Stress in the multilayers was measured with kSA Multiple-beam Optical Sensor (k-Space Associates, Inc., Dexter, MI, USA). The stress was determined using Stoney's equation [37] by measuring changes in the curvature of the samples before and after annealing. Multilayers, which were stored in a cabinet filled with nitrogen gas, were also characterized for their period, microstructure and stress after each annealing step.

Thermal annealing of the first Mo_2C/SiC set was performed in a vacuum furnace with preset heating and cooling cycles at 10^{-7} Pa (HSD Engineering Inc., Oakland, CA, USA). The first Mo_2C/SiC set was annealed to 300°C and 700°C using a slow heating rate (5°C/min). The samples remained at the temperature for 1 hour, after which the heating was turned off. When the temperature was below 80°C, the samples were taken out of the oven. Low-temperature

Optical Materials EXPRESS

annealing of the second set of Mo_2C/SiC multilayers was done in a different oven (DEKEMA, Freilassing, Germany). These were heated to 70, 100, 150, 200, 250, and 300°C at 70 mbar. The heating rate was the same (5°C/min), and samples stayed at each temperature for 1 hour before the heating was turned off and the samples were left to cool down. These samples were also measured for their period, stress, and microstructure after each annealing step. The same oven was used for cycled annealing to 250°C with a fast heating rate (50°C/min).

Monolayers of Mo_2C and SiC were also analyzed with the Rutherford backscattering spectrometry (RBS) using the Van de Graaff accelerator (HZDR, Dresden, Germany). The RBS analysis was performed on as-deposited and annealed (250°C and 700°C for 1 hour) monolayers using 1.7 MeV He^+ beam. These spectra were used to extract information on areal density and any impurities in the coating. Known film thickness and assumed stoichiometry for Mo_2C and SiC allowed us to estimate the volume densities of these coatings. In addition to layer thickness and microstructure, which were measured using SAXRD and HAXRD, we also measured stress.

3.2. Annealing with slow heating rate

The first set of Mo_2/SiC multilayers (period Λ= 5 nm and Γ = 0.3 or 0.5) was used to assess the stability of the multilayers at higher temperatures. Figure 3 shows the results for 5 nm period multilayers with Γ = 0.5 annealed to 300°C and 700°C. Annealing to 300°C resulted in no measurable change in the multilayer period within the error bar (±0.01 nm). Annealing to 700°C resulted in a 1.1% shift in the peak positions towards higher angles, indicating a decrease (contraction) of the multilayer period. This contraction, although small, is not acceptable and would lead to a degradation of the focal spot. Even though annealing to 300°C (Table 2) did not result in any significant period change, stress changed considerably. In the as-deposited state, the multilayers were under compressive (negative) stress. Annealing to 300°C changed the stress to tensile, which became even more tensile at 700°C.

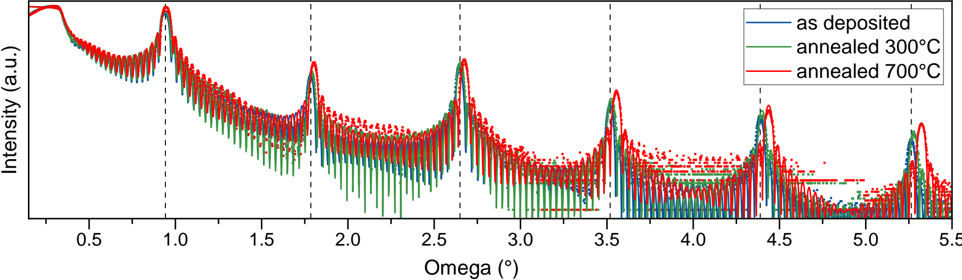

Fig. 3. SAXRD profiles of Mo_2C/SiC multilayers with 5 nm period and Γ = 0.5 in the as-deposited state and after annealing to 300°C and 700°C. The measurements (dots) were fitted (solid line) using IMD software [36]. Dashed vertical lines indicate the positions of the peaks in the as-deposited state.

The second set of Mo_2C/SiC multilayers was used to follow the stress evolution at lower temperatures (from 70 to 300°C) as a function of annealing temperature. We chose to explore this temperature region since numerical simulations predicted that the temperature in MLLs exposed to XFEL pulses with 10 kHz repetition rate under aforementioned conditions (Table 1) should not exceed 300°C. In Fig. 4(a) SAXRD measurements and fits for 5 nm period Mo_2C/SiC multilayer in as-deposited state and after annealing to 100°C, 200°C, 250°C and 300°C are plotted. There are no evident changes observed in the data sets. Figure 4(b) shows a relative change in the multilayer period as a function of the annealing temperature for the multilayers with periods of 1.5, 5, and 12 nm. The gray shaded area indicates the change in the multilayer period of ±0.5%. All data points are within this range except a few points related to multilayers with a period of 1.5

Optical Materials EXPRESS

Table 2. Multilayer period Λ and stress ± standard deviation (SD) for Mo_2C/SiC multilayer before and after annealing to 300℃ and 700℃ for Γ = 0.5 and 0.3

Γ	State	Λ, nm	Stress ± SD, MPa
0.5	as-deposited	5.05	-234 ± 70
	annealed at 300°C	5.04	503 ± 300
	annealed at 700°C	5.00	995 ± 30
0.3	as-deposited	4.98	-410 ± 150
	annealed at 300°C	4.96	520 ± 250
	annealed at 700°C	4.90	960 ± 130

nm. However, for this short-period multilayer, it is also harder to determine the period thickness with the same precision as for the larger-period multilayers. Hence, the error bars are larger.

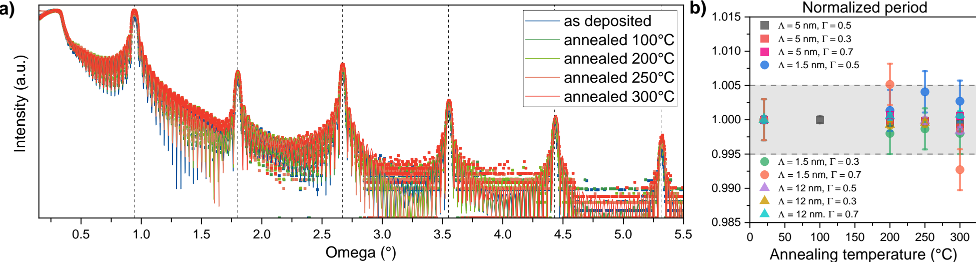

Fig. 4. (a) SAXRD measurements (gray circles) and fits (solid lines) for Mo_2C/SiC multilayer with a period of 5 nm in the as-deposited state and after annealing to 100°C, 200°C, 250°C and 300°C. (b) Normalized multilayer periods as a function of annealing temperature. Data points correspond to different periods and Γ values. The gray band indicates ± 0.5% tolerance.

Figures 5(a-c) show the stress maps in the 2D layer thickness parameter space for Mo_2C/SiC system in the as-deposited state (a) and after annealing for 1 hour at 150°C (b) and 300°C (c) with slow heating rate. Parametric stress plots are based on the stress measurements denoted by white squares. The contours were computed using a linear interpolation followed by smoothing (applying thin plate spline algorithm [38]). Although there is a certain level of approximation associated with the interpolation and errors in the algorithm, the contour plots are helpful in showing the general trends for stress in layer thickness parameter space and for easier comparison before and after annealing. It is especially useful in the context of MLLs, which include a wide range of layer thicknesses. Figures 5(d-f) show stress measurements as a function of annealing temperature (70°C to 300°C) for multilayers with periods of Λ of 1.5, 5, and 12 nm and Γ of 0.3, 0.5, and 0.7.

Stress in the as-deposited Mo_2C/SiC multilayers is thickness-dependent. Short-period multilayers (1.5 nm) have close to zero stress independent of Γ values. In larger-period multilayers, stress is compressive and depends on Γ. Low Γ multilayers, which contain more SiC than Mo_2C, exhibit higher compressive stress than multilayers with high Γ. All multilayers experience stress change, even when annealed to 150°C. The magnitude of the stress change is correlated with the period thickness. For example, the stress in 5 nm multilayers annealed to 150°C changed from compressive to close to zero (Fig. 5(b, e)). Stress in 12 nm multilayers, which was initially about -600 MPa, changed to -400 MPa, while in the 1.5 nm period multilayers,

Optical Materials EXPRESS

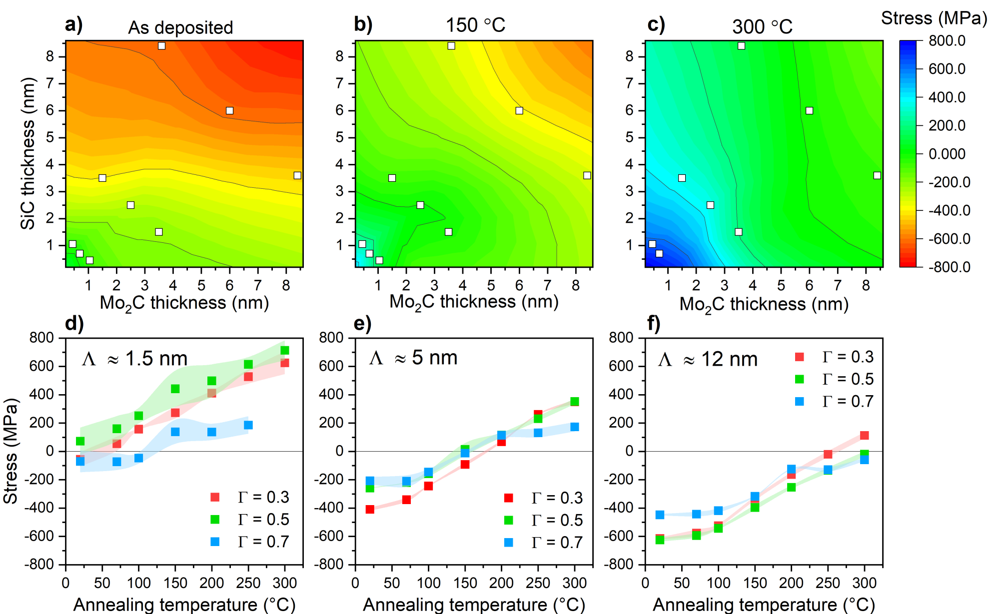

Fig. 5. (a, b, c) Stress contour plots based on stress measurements denoted by white squares in the 2D layer thickness parameter space with Mo_2C layer thickness on the x-axis and SiC layer thickness on the y-axis. Stress values are indicated with colors. Compressive stress is shown in red, close to zero (relaxed) state in green and tensile stress in blue. The stress contours indicate transition from (a) predominantly compressive stress in as-deposited Mo_2C/SiC multilayers to (b) a mixed compressed-relaxed state after annealing to 150°C for 1 hour, and (c) a relaxed-tensile state after annealing to 300°C for 1 hour. (d, e, f) Stress in Mo_2C/SiC multilayer is also shown as a function of annealing temperature (from as-deposited state to 300°C) for multilayer periods of Λ (d) 1.5 nm, (e) 5 nm, and (f) 12 nm and for different Γ ratios. The shaded areas indicate the standard deviation of the stress values across the multilayer samples.

the initially close to zero stress shifted into the tensile regime. Further annealing of 1.5 nm period multilayers to 300°C increased stress to 800 MPa, while the 12 nm period multilayers changed under these conditions into an almost stress-free state.

3.3. Cycled annealing with fast heating rate

Materials exposed to intense XFEL beams experience instantaneous heating, which is hard to reproduce in the laboratory. Hence, the results from thermal annealing tests have to be considered with some reservations. In addition to the annealing experiments reported above, multilayers were also exposed to cycled annealing with a fast heating rate (50°C/min). Only Mo_2C/SiC multilayers with Γ of 0.5 and 0.3 and periods of 1.5, 5, and 12 nm were tested this way. Each multilayer underwent 35 heating-cooling cycles, with each cycle lasting about 30 minutes. In a single cycle, the multilayer was heated to 250°C with a heating rate of 50°C/min. The multilayer stayed at this temperature for 5 min and was then cooled down in the air for about 20 minutes. The choice of 250°C was based on the numerical simulation results (Table 1 and Fig. 2). The total cycled annealing time for 35 cycles was 17.5 hours.

Samples were measured only after the full completion of 35 heating-cooling cycles. Figure 6(a) shows SAXRD scans of 5 nm and Γ = 0.5 multilayer before (bottom) and after (top) annealing. Stress values are plotted in Fig. 6(c) and also listed in Table 3. Due to the faster heating rate, it

was harder to ensure that the maximum temperature would not go beyond 250°C. Based on the logfile the maximum temperature was often above 250°C to as high as 280°C. Also, after 20 minutes of cooling in the air, the temperature in the oven was still close to 150°C. So, realistically, the sample was exposed to 35 heating-cooling cycles where the temperature varied between 150°C and 280°C.

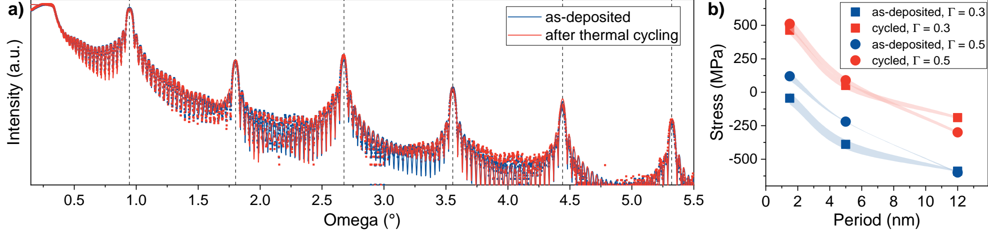

Fig. 6. (a) SAXRD profiles for 5 nm period sample with Γ = 0.5 in the as-deposited state after cycled annealing to 250°C. (b) Stress as a function of the period for as-deposited and thermally cycled multilayers with Γ = 0.3 and 0.5.

Table 3. Mo_2C/SiC multilayer period Λ and stress ± standard deviation (SD) for 1.5, 5 and 12 nm period multilayers and Γ = 0.5 and 0.3 for two sample sets: AD - as-deposited, SA 300°C - annealing at 300°C with a slow heating rate (5°C/min), cycled - cycled annealing to 250°C with faster heating rate (50°C/min)

	Sample set 2						Sample set 3			
Γ	0.3			0.5			0.3		0.5	
State	AD	SA 300°C	cycled	AD	SA 300°C	cycled	AD	cycled	AD	cycled
Λ, nm	1.50	1.50	1.50	1.47	1.48	1.48	1.49	1.49	1.48	1.48
Stress, MPa	-60	630	610	70	710	690	-45	460	120	510
Stress SD	± 50	± 80	± 40	± 100	± 70	± 90	± 45	± 30	± 30	± 40
Γ	0.3			0.5			0.3		0.5	
State	AD	SA 300°C	cycled	AD	SA 300°C	cycled	AD	cycled	AD	cycled
Λ, nm	4.99	4.99	4.99	5.00	5.00	4.99	4.97	4.97	5.00	5.00
Stress, MPa	-410	350	320	-260	350	350	-390	50	-260	90
Stress SD	± 10	± 10	± 10	± 5	± 20	± 10	± 35	± 25	± 5	± 20
Γ	0.3			0.5			0.3		0.5	
State	AD	SA 300°C	cycled	AD	SA 300°C	cycled	AD	cycled	AD	cycled
Λ, nm	11.84	11.81	11.81	11.92	11.90	11.91	11.87	11.86	11.90	11.90
Stress, MPa	-610	110	115	-620	-20	-30	-590	-190	-600	-300
Stress SD	± 10	± 20	± 20	± 10	± 20	± 20	± 5	± 10	± 5	± 10

Interestingly, even though the total annealing time in these cycled annealing experiments was longer (175 minutes at maximum temperature) and the maximum temperature was slightly higher (280°C), the multilayers exhibited smaller changes in their period and stress as compared to multilayers annealed with slow heating rate, which stayed at 250°C for 1 hour. In fact, changes in the stress of the former were comparable to multilayers annealed to 200°C with a slow heating rate. It is intriguing that this temperature matches the average temperature during the cycled annealing.

Finally, we tested if and how does the stress in multilayers cured at 300°C change if these multilayers are heated again to the temperatures below 300°C. For this purpose we performed cycled annealing to 250°C on the second sample set, which was previously heated to 300°C. We

Optical Materials EXPRESS

monitored both stress and period and observed no changes. Both remained stable within the error bars of the measurements (see Table 3, Sample set 2).

The HAXRD data of the 12 nm period Mo_2C/SiC multilayers and $\Gamma = 0.3, 0.5$ and 0.7 are shown in Fig. 7(a), (b) and (c), respectively. One can see that higher Mo_2C content is associated with a stronger peak centered at around 2θ of 41°. The asymmetric shape of the peak suggests an overlap of two neighboring reflections located at 38° and 41.5°, also observed in HAXRD spectra of Mo/C multilayers with very thin (0.5 nm) C layers [24]. These diffraction peaks are indicative of (002) and (101) of hexagonal β-Mo_2C phase at 37.5° and 39.6°, respectively [39]. The slight shift of the peaks towards higher 2θ values can be associated with defects or compositional variations of Mo_2C. No change in the intensity or in the shape of these peaks could be observed due to annealing, independent of how the annealing was performed (Fig. 7). As expected, in multilayers with Mo_2C layer thickness of less than 3 nm, this diffraction peak is barely noticeable and very broad, indicating close to amorphous Mo_2C. With the increasing thickness the peak intensity is getting higher. However, based on Scherrer equation [40], the Mo_2C crystals are considerably smaller than Mo_2C layer thickness. In the case of a 12 nm period multilayer, for example, with 8.4 nm Mo_2C thick layers, these crystals are smaller than 2.7 nm.

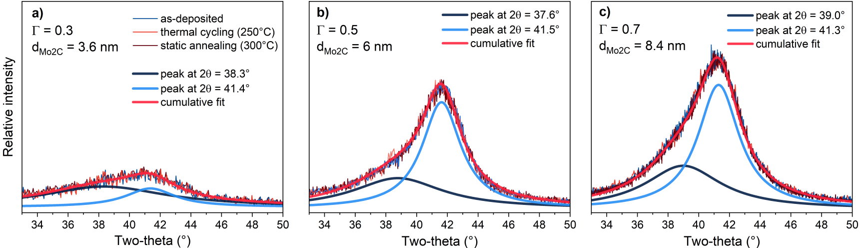

Fig. 7. HAXRD data of Mo_2C/SiC multilayers with a period of 12 nm (a) $\Gamma = 0.3$, (b) $\Gamma = 0.5$, and (c) $\Gamma = 0.7$ of as-deposited, cycled annealed with fast heating rate and annealed with slow heating rate. The multilayers with higher content of Mo_2C (larger Γ) show a more prominent diffraction peak centered at 41°. The asymmetric shape suggests that it most likely consists of two peaks, as illustrated by the multi-peak fit.

4. Discussion

In this study, we investigated multilayer candidates for MLLs to be used for focusing XFEL beams. High peak brilliance of XFELs sets strict limits on the choice of materials for MLLs: they should be low-absorbing, thermally stable, and able to form smooth layers with sharp and stable interfaces. Given the anticipated high diffraction efficiency of Mo_2C/SiC and previous reports on Mo/Si and Mo_2C/Si multilayers [24,41] we chose to investigate Mo_2C/SiC.

To assess the thermal behavior of MLLs made of Mo_2C/SiC, we first conducted numerical simulations of the heat load they would experience under XFEL beams of 17.5 keV photon energy and 1 mJ per pulse energy, with repetition rates of 10 kHz and 0.27 MHz. In these simulations, the multilayer structure was modeled as a slab made of two materials in the proportion indicated by Γ. Hence, we approximated the thermal properties of the multilayer structure as the average of the individual components and then used them to predict the temperature rise in the MLLs under specific XFEL beam conditions. Using this approach, we predicted that the temperature in MLLs exposed to an XFEL beam with a repetition rate of 10 kHz would stay below 300°C. However, a higher repetition rate of 0.27 MHz (3.6 μs between pulses) would heat the MLLs to 2000°C.

Using the temperature predicted by the numerical simulations as our benchmark, we conducted annealing studies to test the thermal stability of Mo_2C/SiC multilayers with different Mo_2C to SiC ratios ($\Gamma = 0.3, 0.5, 0.7$) and periods (1.5 nm, 5 nm, 12 nm). Annealing multilayers to

Optical Materials EXPRESS

300°C resulted in no significant changes while annealing to 700°C led to unacceptable changes in the multilayer period as well as to a change in stress from compressive to high tensile stress approaching 1 GPa. Thus, MLLs based on Mo_2C/SiC multilayers are not suited for focusing XFEL beams with a repetition rate much higher than 10 kHz.

Our stress investigations revealed that the stress in Mo_2C/SiC multilayers in the as-deposited state depends on the multilayer period and Γ. However, as compared to Mo/Si [24] where stress for different Γ spans from compressive to tensile (e.g. -400 MPa, 0, 600 MPa for Γ of 0.3, 0.5 and 0.7 for 5 nm period multilayer) stress in same period Mo_2C/SiC multilayers stays compressive (-390 MPa, -260 MPa, -210 MPa) for Γ 0.3, 0.5, and 0.7, respectively. The larger content of Mo in Mo/Si multilayers shifts stress significantly into a tensile direction while the effect of Mo_2C is much smaller. Previous study of Mo_2C/Si multilayers also indicated that the stress in Mo_2C-based multilayers is more compressive than in Mo/Si [35].

Similarly to Mo/Si multilayers [24], we observe period thickness-dependent stress behavior, with thicker period multilayers associated with higher compressive stress. For instance, 1.5 nm period multilayers are almost stress-free, while 12 nm multilayers are in compressive stress, reaching -600 MPa. This compressive stress is likely introduced during deposition and can be related to volume changes induced by the energetic bombardment of incident adatoms, in our case Kr, and associated ions, along with interfacial contraction or expansion-induced stresses. This phenomenon leads to substantial compressive stresses, often referred to as the 'atomic peening' effect [24,42], which can cause the churning of atoms within 1 - 1.5 nm of the surface [43]. Consequently, the resulting compressive stress increases as thicker layers experience prolonged bombardment by energetic atoms and ions.

Annealing of Mo_2C/SiC multilayers changes stress from compressive to tensile. It is interesting that the shift in stress for the same annealing temperature is similar and independent of the multilayer period. For example, annealing of 1.5, 5 and 12 nm period multilayers to 300°C shifts the stress on average by 600 MPa. With increasing temperature stress continues to increase. For example, stress in 5 nm period Mo_2C/SiC multilayers with $\Gamma = 0.3$ and $\Gamma = 0.5$ increased to 1000 MPa when annealed to 700°C (see Table 2). Assuming steady stress increase with temperature this corresponds to about 2 MPa/°C.

The stress evolution of Mo_2C/SiC as a function of temperature is similar to Mo/Si and Mo_2C/Si systems. In Mo/Si [44] and Mo_2C/Si [35,45] multilayers it was demonstrated that temperature-induced stress-relaxation predominantly occurs in the Si layers through viscous flow associated with defect annihilation in the amorphous silicon layers [35,44]. The relaxation of stress in Mo_2C/SiC multilayers is likely governed by the same mechanism but happens at a lower temperature. For Mo/Si multilayers, stress relaxation for a multilayer with a period of 6.4 nm occurs at 310°C, while in Mo_2C/Si this happens already at 280°C [45]. In Mo_2C/SiC multilayers (5 nm period), where both materials consist of carbides, stress relaxed already at 150°C for $\Gamma = 0.5$ and 0.7. Based on our data, we predict that zero stress for 5 nm period and $\Gamma = 0.3$ Mo_2C/SiC multilayers should occur at 180°C. Larger period multilayers (12 nm) undergo relaxation upon thermal annealing to 250°C for $\Gamma = 0.3$ and 300°C for $\Gamma = 0.5$ and $\Gamma = 0.7$. Annealing the multilayer to achieve close to zero stress might be beneficial before cutting MLLs out of it.

In this study, we also investigated the effect of different heating rates. Stress changes in multilayers annealed to 250°C in cycled annealing with a fast heating rate resembled stress changes obtained at a lower annealing temperature (200°C) with a slow heating rate. We also demonstrated that multilayers annealed to 300°C remained stable in period and stress if subsequently exposed to a lower temperature. Hence, curing the multilayers at a temperature above the target temperature is beneficial to stabilize the multilayers.

HAXRD measurements of Mo_2C/SiC multilayers indicate no changes in the microstructure of Mo_2C as a function of period thickness or annealing temperature. Only in multilayers with

Optical Materials EXPRESS

larger Γ (e.g. 0.7), which are, however, of less interest because of the larger content of high Z material, a broad peak between 37° and 43° appears, which indicates an onset of crystallite formation (β-Mo_2C hexagonal phase). As a side study, we investigated HAXRD spectra of thick (86 nm) Mo_2C monolayers. In the as-deposited state (see Fig. 8(a)), two peaks were identified between 36° and 39°, similar to what was observed in 12 nm multilayers (Fig. 7). In the multilayer, these peaks were much broader since the Mo_2C layers were substantially thinner (the thickest was 8.4 nm for Γ = 0.7). In the Mo_2C monolayer, the two peaks can be identified as (002) and (101) reflections corresponding to β-Mo_2C phase (PDF35-0787). Interestingly, annealing the monolayer to 250°C results in the disappearance of these peaks, indicating a transition to an amorphous state. Further annealing results in the amorphous-to-crystalline transition. Monolayer annealed to 700°C shows two distinct peaks at 34.47° and 39.53° identified as (021) and (121) characteristic for orthorhombic α-Mo_2C phase (PDF72-1683). This phase was observed before in monolayers deposited with magnetron sputtering and annealed to 700°C [39]. Such transformations are most likely associated with a change in stress and could possibly result in density change. In contrast, HAXRD profiles of thick SiC monolayer indicate that SiC is amorphous in the as-deposited state and after annealing up to 700°C. Mo_2C monolayers in the as-deposited state are essentially stress-free. When heated the stress is shifting towards tensile. SiC monolayers are highly compressive in the as-deposited state (stress -930 MPa) but also become tensile after annealing. Based on this, one could speculate that the compressive stress in as-deposited Mo_2C/SiC multilayers of the larger period (5 nm and 12 nm) is mostly due to highly compressive SiC layers.

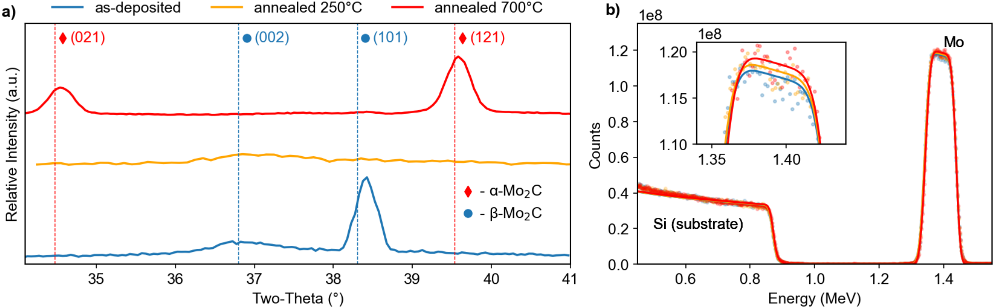

Fig. 8. Mo_2C monolayers with a thickness of 86.3 ± 0.5 nm in the as-deposited state (blue) and after annealing to 250°C (orange) and 700°C (red): (a) HAXRD data, (b) RBS spectra.

Finally, we wanted to investigate if annealing has any effect on the density of Mo_2C and SiC. Table 4 lists the monolayer thicknesses determined from SAXRD fits along with RBS results. Volume density was computed based on the film thickness, assumed stoichiometry, and areal atomic density (at/cm^2) for each monolayer. Within the error bars, the densities of both materials show no change due to annealing. RBS results indicated higher than assumed carbon content in as-deposited Mo_2C. In the annealed sample, carbon was reduced by 0.3%. Figure 8(b) shows the RBS spectra for Mo_2C monolayers, which exhibit no sign of impurities.

Optical Materials EXPRESS

Table 4. Thickness, stoichiometry, and mass density of Mo_2C and SiC monolayers determined from SAXRD and RBS analyses

Material	State	Thickness, nm	Assumed stoichiometry	Density, g/cm^3
Mo_2C	as-deposited	86.3 ± 0.5	$Mo_{0.528}C_{0.472}$	8.3 ± 0.1
	annealed 250°C	86.3 ± 0.5	$Mo_{0.532}C_{0.468}$	8.3 ± 0.1
	annealed 700°C	86.5 ± 0.5	$Mo_{0.531}C_{0.469}$	8.1 ± 0.1
SiC	as-deposited	99 ± 0.7	$Si_{0.436}C_{0.564}$	2.97 ± 0.05
	annealed 250°C	99 ± 0.7	$Si_{0.435}C_{0.565}$	2.90 ± 0.05
	annealed 700°C	99 ± 0.7	$Si_{0.423}C_{0.577}$	2.87 ± 0.05

5. Summary

In this work, we explored possible multilayer material pairs that could be used for preparing more robust MLLs for XFEL applications. Numerical simulations of heat loads led us to focus on low-density material pairs. After preliminary screening we studied Mo_2C/SiC in more detail. Based on the results presented here we conclude that the Mo_2C/SiC multilayer system is a viable option for MLLs to focus an XFEL beam of 1 mJ per pulse energy and a repetition rate of 10 kHz, parameters we plan to use in our upcoming beamtime at European XFEL. The annealing experiments, which are usually a good indicator for multilayer stability, indicate that MLLs made of Mo_2C/SiC multilayers are expected to withstand these conditions with no deterioration of their focusing performance.

Funding. Slovenian Research and Innovation Agency (ARIS) (J2-4477, P2-0162); Deutsche Forschungsgemeinschaft (EXC 2056 – project ID 390715994).

Acknowledgments. We thank Sabrina Bolmer and Harumi Nakatsutsumi for technical support. M.Z. would like to thank Mauro Prasciolu for his valuable advice throughout the annealing study. We acknowledge DESY (Hamburg, Germany), a member of the Helmholtz Association HGF, for the provision of experimental facilities. Parts of this research were carried out at the Ion Beam Center at the Helmholtz-Zentrum Dresden - Rossendorf e. V., a member of the Helmholtz Association. We would like to thank Dr. René Heller for his assistance with measurements. This work was partly funded by the Cluster of Excellence "CUI: Advanced Imaging of Matter" of the Deutsche Forschungsgemeinschaft (DFG)–EXC 2056–project ID 390715994 and by the Center for Free-Electron Laser Science (CFEL) under the project: Innovative methods for imaging with the use of x-ray free-electron laser (XFEL) and synchrotron sources: simulation of gas-focused micro-jets, and Slovenian Research and Innovation Agency (ARIS) - projects P2-0162 and J2-4477.

Disclosures. The authors declare no conflicts of interest.

Data availability. Data underlying the results presented in this paper are not publicly available at this time but may be obtained from the authors upon reasonable request.

References

1. H. N. Chapman, "X-ray free-electron lasers for the structure and dynamics of macromolecules," Annu. Rev. Biochem. **88**(1), 35–58 (2019).
2. R. Schoenlein, T. Elsaesser, and K. Holldack, "Recent advances in ultrafast X-ray sources," Phil. Trans. R. Soc. A. **377**(2145), 20180384 (2019).
3. C. Pellegrini, "X-ray free-electron lasers: from dreams to reality," Phys. Scr. **2016**, 014004 (2017).
4. I. Bahns, P. Rauer, and J. Rossbach, "Thermoelastic effects in Bragg reflectors as a potential bottleneck for XFELs with megahertz repetition rate," Commun. Phys. **7**(1), 95 (2024).
5. P. Heimann, M. MacDonald, and B. Nagler, "Compound refractive lenses as prefocusing optics for X-ray FEL radiation," J. Synchrotron Radiat. **23**(2), 425–429 (2016).
6. K. Yamauchi, M. Yabashi, and H. Ohashi, "Nanofocusing of X-ray free-electron lasers by grazing-incidence reflective optics," J. Synchrotron Radiat. **22**(3), 592–598 (2015).
7. C. David, S. Gorelick, and S. Rutishauser, "Nanofocusing of hard X-ray free electron laser pulses using diamond based Fresnel zone plates," Sci. Rep. **1**(1), 57 (2011).
8. S. Matsuyama, T. Inoue, and J. Yamada, "Nanofocusing of X-ray free-electron laser using wavefront-corrected multilayer focusing mirrors," Sci. Rep. **8**(1), 17440 (2018).
9. M. Prasciolu, K. T. Murray, v Ivanov, *et al.*, "On the use of multilayer Laue lenses with X-ray free electron lasers," in *International Conference on X-Ray Lasers 2020*, vol. 11886 (SPIE, 2021), pp.159–166.

Optical Materials EXPRESS

10. H. Yan, V. Rose, and D. Shu, "Two dimensional hard x-ray nanofocusing with crossed multilayer Laue lenses," Opt. Express **19**(16), 15069–15076 (2011).
11. S. Bajt, M. Prasciolu, and H. Fleckenstein, "X-ray focusing with efficient high-NA multilayer Laue lenses," Light: Sci. Appl. **7**(3), 17162 (2017).
12. M. Prasciolu, A. F. G. Leontowich, and J. Krzywinski, "Fabrication of wedged multilayer Laue lenses," Opt. Mater. Express **5**(4), 748–755 (2015).
13. H. N. Chapman, M. Prasciolu, and K. T. Murray, "Analysis of X-ray multilayer Laue lenses made by masked deposition," Opt. Express **29**(3), 3097–3113 (2021).
14. A. T. Macrander, A. Kubec, and R. Conley, "Efficiency of a multilayer-Laue-lens with a 102 μm aperture," Appl. Phys. Lett. **107**(8), 081904 (2015).
15. H. C. Kang, G. B. Stephenson, and C. Liu, "Sectioning of multilayers to make a multilayer Laue lens," Rev. Sci. Instrum. **78**(4), 046103 (2007).
16. Z. Rek, H. N. Chapman, B. Šarler, *et al.*, "Numerical simulation of heat load for multilayer Laue lens under exposure to XFEL pulse trains," Photonics **9**(5), 362 (2022).
17. I. Bahns, P. Rauer, J. Rossbach, *et al.*, "Stability of Bragg reflectors under megahertz heat load at XFELs," J. Synchrotron Radiat. **30**(1), 1–10 (2023).
18. S. Bajt, H. N. Chapman, A. Aquila, *et al.*, "High-efficiency x-ray gratings with asymmetric-cut multilayers," J. Opt. Soc. Am. A **29**(3), 216–230 (2012).
19. H. Yan, R. Conley, N. Bouet, *et al.*, "Hard x-ray nanofocusing by multilayer Laue lenses," J. Phys. D: Appl. Phys. **47**(26), 263001 (2014).
20. A. Authier, *Dynamical Theory of X-Ray Diffraction*, International Union of Crystallography Monographs on Crystallography (Oxford University Press, 2001).
21. T. Schoonjans, A. Brunetti, and B. Golosio, "The xraylib library for x-ray-matter interactions. Recent developments," Spectrochim. Acta, Part B **66**(11-12), 776–784 (2011).
22. C. Liu, R. Conley, and A. T. Macrander, "Film stress studies and the multilayer Laue lens project," in *Advances in X-Ray/EUV Optics, Components, and Applications*, vol. 6317 (SPIE, 2006), pp. 151–159.
23. D. L. Windt, W. L. Brown, C. A. Volkert, *et al.*, "Variation in stress with background pressure in sputtered Mo/Si multilayer films," J. Appl. Phys. **78**(4), 2423–2430 (1995).
24. D. L. Windt, "Stress, microstructure, and stability of Mo/Si, W/Si, and Mo/C multilayer films," J. Vac. Sci. Technol., A **18**(3), 980–991 (2000).
25. D. L. Windt and J. A. Bellotti, "Performance, structure, and stability of SiC/Al multilayer films for extreme ultraviolet applications," Appl. Opt. **48**(26), 4932–4941 (2009).
26. A. Andrejczuk, J. Krzywinski, and S. Bajt, "Influence of imperfections in a wedged multilayer Laue lens for the focusing of X-rays investigated by beam propagation method," Nucl. Instrum. Methods Phys. Res., Sect. B **364**, 60–64 (2015).
27. K. Liao, Y. Hong, and Q. Wang, "Analysis of tilted multilayer Laue lens with stochastic layer thickness error," Opt. Commun. **325**, 111–115 (2014).
28. C. P. Jensen, K. K. Madsen, and F. E. Christensen, "Small d-Spacing WC/SiC multilayers for future hard X-ray telescope designs," Experimental Astronomy **20**(1-3), 93–103 (2006).
29. M. Fernández-Perea, M. J. Pivovaroff, and R. Soufli, "Ultra-short-period WC/SiC multilayer coatings for x-ray applications," Nucl. Instrum. Methods Phys. Res., Sect. A **710**, 114–119 (2013).
30. K. T. Murray, A. F. Pedersen, and I. Mohacsi, "Multilayer Laue lenses at high X-ray energies: performance and applications," Opt. Express **27**(5), 7120–7138 (2019).
31. S. Bajt, J. B. Alameda, and T. W. B. Jr, "Improved reflectance and stability of Mo/Si multilayers," Opt. Eng. **41**(8), 1797–1804 (2002).
32. S. Braun, H. Mai, and M. Moss, "Mo/Si multilayers with different barrier layers for applications as extreme ultraviolet mirrors," Jpn. J. Appl. Phys. **41**(Part 1, No. 6B), 4074 (2002).
33. H. Takenaka and T. Kawamura, "Thermal stability of Mo/C/Si/C multilayer soft X-ray mirrors," J. Electron Spectrosc. Relat. Phenom. **80**, 381–384 (1996).
34. S. Bajt, D. G. Stearns, and P. A. Kearney, "Investigation of the amorphous-to-crystalline transition in Mo/Si multilayers," J. Appl. Phys. **90**(2), 1017–1025 (2001).
35. T. D. Nguyen, T. W. B. Jr, L. Chrostowski, *et al.*, "Residual stresses in Mo/Si and Mo_2C/Si multilayers," in *X-Ray Optics, Instruments, and Missions*, vol. 3444 (SPIE, 1998), pp. 543–550.
36. D. L. Windt, "IMD-Software for modeling the optical properties of multilayer films," Comput. Phys. **12**(4), 360–370 (1998).
37. G. G. Stoney, "The tension of metallic films deposited by electrolysis," Proceedings of the Royal Society of London. Series A **82**, 172–175 (1909).
38. G. Donato and S. Belongie, "Approximate thin plate spline mappings," in *Computer Vision - ECCV 2002* A. Heyden, eds. (Springer Berlin Heidelberg, 2002), pp. 21.
39. Z. Wu, J. Zhao, and M. Zhu, "Effects of film thickness and annealing temperature on the properties of molybdenum carbide films prepared using pulsed direct-current magnetron sputtering," Mater. Res. Express **9**(2), 026403 (2022).
40. A. L. Patterson, "The Scherrer formula for X-ray particle size determination," Phys. Rev. **56**(10), 978–982 (1939).

Optical Materials EXPRESS

41. T. D. Nguyen and J. H. Underwood, "Stress, microstructure, and thermal behavior in Mo/Si X-ray multilayers," Mater. Res. Soc. Symp. Proc. **382**, 297 (1995).
42. F. D'Heurle and J. Harper, "Note on the origin of intrinsic stresses in films deposited via evaporation and sputtering," Thin Solid Films **171**(1), 81–92 (1989).
43. M. Hasan, R. Highmore, and R. Somekh, "The UHV deposition of short-period multilayers for X-ray mirror applications," Vacuum **43**(1-2), 55–59 (1992).
44. R. R. Kola, D. L. Windt, and W. K. Waskiewicz, "Stress relaxation in Mo/Si multilayer structures," Appl. Phys. Lett. **60**(25), 3120–3122 (1992).
45. T. Feigl, S. Yulin, T. Kuhlmann, *et al.*, "Damage resistant and low stress EUV multilayer mirrors," Jpn. J. Appl. Phys. **41**(Part 1, No. 6B), 4082 (2002).

178.79.95.172 {ts 2024-12-20 05:41:47}